Available online at http://www.cnki.net

The Journal of China Universities of Posts and Telecommunications

April 2020, 27(2): 10 – 18

http://jcupt.bupt.edu.cn

Interference suppression for ultra dense network based on compressive sensing framework

Hou Huanhuan(✉), Jiang Jing, Lei Ming, Liu Ben

School of Communications and Information Engineering, Xi'an Universityof Posts and Telecommunications, Xi'an 710061, China

Abstract

Ultra-dense network (UDN) deployment of small cells introduces novel technical challenges, one of which is that the interference levels increase considerably with the network density. This paper proposes interference suppression scheme based on compressive sensing (CS) framework for UDN. Firstly, the measurement matrix is designed by exploiting the sparsity of millimeter wave channels. CS technique is employed to transform the high dimension sparse signal into low dimension signal. Then, the interference is canceled in the compressed domain. Finally, the stagewise weak orthogonal matching pursuit (SWOMP) algorithm is used to reconstruct the useful signal after interference suppression. The analysis and simulation results demonstrate the effectiveness of the algorithm. Simulation results demonstrate that the proposed interference suppression in compressive domain yields performance gains compared to other classical interference suppression schemes. The proposed algorithm can reduce the computational complexity of interference suppression algorithm.

Keywords interference suppression, CS, signal reconstruction, UDN

1 Introduction

UDN has been considered as the key feature to meet the ever-increasing demand of high-data-rate applications in 5G mobile communication system [1 – 3]. The deployment of ultra dense cell is that the access nodes are as close as possible to the end users, thus achieving a possible high transmission rate. However, the system capacity of UDN is not necessarily proportional to cell density. As densification, interference is the main bottle neck of the performance improvement [4 – 5].

The interference suppression of UDN is mainly classified as three types, cell clustering, interference management and coordinated multi-points (CoMP) transmission [6 – 8]. With denser cells, the number of interference source increases greatly. It means that the interference suppression shall involve more cells across the network. The traditional interference suppression technologies become more complicate. Moreover, the system performance is degraded with the increase of interference cells [3 – 5]. On the other hand, the femto cells are unplanned and user-deployment in UDN, collaborative transmission technology is difficult to achieve due to the lack of the central point. Refs. [9 – 11] put forward user-centric clustering and cooperating transmission for UDN. However, it is difficult to cope with the dramatic changes in the transmission data rate and cell on/off.

Received date: 06-08-2018

Corresponding author: Hou Huanhuan, E-mail: houhh321@163.com

DOI: 10.19682/j.cnki.1005-8885.2020.1002

Thus, the novel interference suppression is needed to investigate UDN scenarios.

The compressed domain interference suppression is mainly used in radar multi-target interference suppression, which can eliminate interference in the compressed domain and improve signal reception quality. Ref. [12] proposes an efficient compressive domain filtering algorithm that eliminates signal interference by exploiting orthogonal projection while preserving the geometry of the set of possible signals of interest. Based on this, Ref. [13] investigates the achievable restricted isometry constant (RIC) of the effective sensing matrix, namely, the product of the orthogonal projection matrix and the original sensing matrix. According to the impact of RIC on signal reconstruction, an improved signal reconstruction algorithm is proposed. Ref. [14] proposes a CS-based approach for narrow band interference suppression in multiple-input multiple-output (MIMO)-orthogonal frequency division multiplexing (OFDM).

For an UDN with a large amount of interference, the sparsity of the wireless channel or the transmission signals can be utilized to transform the interference signal into the compressed domain, reducing the dimension of the interference signal and then filtering the interference. Therefore, interference suppression in the compressed domain can solve the problem of a large number of interference sources in ultra-dense networking, and improve the interference suppression performance of ultra-dense interference sources. Ref. [15] considers that uplink data in centralized radio access networks (C-RANs) and narrow-band interference (NBI) from other systems are sparse in some application scenarios, and joint NBI mitigation and data recovery problems can be naturally formulated as CS problems. Ref. [16] considers the number of base station (BS) with unique identities can be quite large in a heterogeneous cellular network, but the actual number of interfering BS is relatively few. By exploiting the sparsity, it shows that finding the identities of constituent BS in the received signal can be solved using block sparse signal reconstruction algorithms. These related works have proposed interference suppression by utilizing CS techniques in heterogeneous network systems. However, the interference compression for UDN scenarios with complex and large interference sources has not been studied.

The compressive domain interference suppression is used in Radar, NBI system or C-RAN based on the above Refs. [12 – 16]. For UDN, the channel characters and signals are completely different from the above scenarios. We consider a heterogeneous network in which ultra-dense small BSs exploit mmWave massive MIMO for access and backhaul, while macro-cell BS provides the control service with low frequency band. The compressive domain interference suppression is applied to cancel the interference caused by a large number of adjacent cells. The major contributions of this paper can be listed as follows.

To avoid the performance degradation due to a large number of interference cells, we propose the interference suppression algorithm based on CS framework in UDN. The measurement matrix and sparse matrix are designed by exploiting the sparsity of millimeter wave channels. Considering that the sparsity of objective signals are different with the interfering signals, the interference in the non-zero value of objective signals is far less than the original signals. We therefore resort to compression sampling tools. The compression sampling transforms the interference and objective signals from high dimension to low dimension in compression domain. After reducing the dimensions of the received signal, a large number of interference is filtered more efficiently in the compressed domain. Base on this, we can acquire and reconstruct a desired signal using far fewer measurements than traditional methods. Since the compressed signal dimension is much smaller than the original signal dimension, the proposed algorithm reduces the computational complexity of interference suppression algorithms.

Moreover, the proposed algorithm can be carried out directly by the transmitter or the receiver, and it does not need coordinated transmission or resource scheduling among multiple cells. By canceling the interference in the compressed domain, we can suppress a large number of interference sources more efficiently and significantly improve the performance of

interference suppression for UDN systems.

Finally, the performance of the compressive domain interference suppression is compared with various reconstruction algorithms. Simulation results demonstrate that the proposed algorithm yields obvious performance gains.

The rest of this paper is organized as follows. Sect. 2 introduces the system model considering the intra-cell and inter-cell interference in UDN. The design of the sparse channel model is presented in Sect. 3. The interference suppression based on CS is formulated in Sect. 4. Sect. 5 provides the performance analysis of our proposed algorithms via simulations and the conclusion is given in Sect. 6. The symbols used in the paper are denoted in Table 1.

Table 1 List of notations

Notation	Description
$(\cdot)^{-1}$	The inverse of a matrix
$(\cdot)^{\mathrm{T}}$	The matrix transpose
$(\cdot)^{\mathrm{H}}$	The matrix conjugate transpose
$(\cdot)^{*}$	The matrix conjugate operations
$\otimes$	The Kronecker product and symbol
$\oplus$	The subspace direct sum operator
$\lvert\cdot\rvert$	The modulus of the matrix

2 System model

Consider UDN system model consisting of M cells, where each cell has one BS with N_t antennas and K mobile stations (MSs) with N_r antennas. Assume that each MS receives N_s streams, KN_s streams are transmitted from BS for downlink. If $\boldsymbol{H}_{mk}$ denotes the $N_r \times N_t$ downlink channel from BS m to user k in cell c, then the received signal at user k in cell c can be written as

$$\boldsymbol{y}_{ck} = \sum_{m=1}^{M} \boldsymbol{H}_{mck}\boldsymbol{F}_m\boldsymbol{x}_m + \boldsymbol{n}_{ck} \tag{1}$$

where $\boldsymbol{x}_m = [\boldsymbol{x}_{m,1}, \ldots, \boldsymbol{x}_{m,k}]^{\mathrm{T}}$ is the $KN_s \times 1$ vector of transmitted symbols from BS m, satisfying $E[\boldsymbol{x}_m\boldsymbol{x}_m^{*}] = (P/KN)\boldsymbol{I}_{KN_s}$, with P representing the average total transmitted power. Each BS $m = 1, 2, \ldots, M$ applies an $N_t \times KN_s$ precoder $\boldsymbol{F}_m = [\boldsymbol{F}_{m,1}, \ldots, \boldsymbol{F}_{m,k}]$ to transmit a symbol for each user. $\boldsymbol{n}_{ck} \in \mathcal{CN}(0, \sigma^2\boldsymbol{I})$ is the Gaussian noise at user k in cell c. $\mathcal{CN}(0, \sigma^2\boldsymbol{I})$ represents the zero-mean complex Gaussian distribution with covariance matrix $\sigma^2\boldsymbol{I}$, $\boldsymbol{I}$ is the unit matrix. It is useful to expand Eq. (1) as

$$\boldsymbol{y}_{ck} = \underbrace{\boldsymbol{H}_{cck}\boldsymbol{F}_{c,k}\boldsymbol{x}_{c,k}}_{\text{Desired signal}} + \underbrace{\sum_{n=1,n\neq k}^{K} \boldsymbol{H}_{cck}\boldsymbol{F}_{c,n}\boldsymbol{x}_{c,n}}_{\text{Intra-cell interference}} + \underbrace{\sum_{m=1,m\neq c}^{M} \boldsymbol{H}_{mck}\boldsymbol{F}_m\boldsymbol{x}_m}_{\text{Inter-cell interference}} + \boldsymbol{n}_{ck} \tag{2}$$

The resulting signal to interference and noise ratio (SINR) of user k used to obtain the spectral efficiency with Shannon's formula is thus given as follows

$$\mathrm{SINR}_k = \frac{\lvert \boldsymbol{H}_{cck}\boldsymbol{F}_{c,k} \rvert^2}{\lvert \underbrace{\sum_{n=1,n\neq k}^{K} \boldsymbol{H}_{cck}\boldsymbol{F}_{c,n}}_{\text{Intra-cell interference}} \rvert^2 + \lvert \underbrace{\sum_{m=1,m\neq c}^{M} \boldsymbol{H}_{mck}\boldsymbol{F}_m}_{\text{Inter-cell interference}} \rvert^2 + \lvert \boldsymbol{n}_{ck} \rvert^2} \tag{3}$$

where $\lvert \boldsymbol{H}_{cck}\boldsymbol{F}_{c,k} \rvert^2$ is the desired signal power, $\left| \sum_{n=1,n\neq k}^{K} \boldsymbol{H}_{cck}\boldsymbol{F}_{c,n} \right|^2$ is the intra-cell multi-user interference power, $\left| \sum_{m=1,m\neq c}^{M} \boldsymbol{H}_{mck}\boldsymbol{F}_m \right|^2$ is the inter-cell interference power, and $\lvert \boldsymbol{n}_{ck} \rvert^2$ is the noise signal power.

3 Channel model

Since mm Wave channels are expected to have limited scattering [17 - 18], we adopt a geometric channel model with L scatters. Each scatterer is further assumed to contribute a single propagation path between the BS and MS. Under this model, the channel $\boldsymbol{H}_{mck}$ can be expressed as

$$\boldsymbol{H}_{mck} = \sqrt{\frac{N_t N_r}{\rho}} \sum_{l=1}^{L} \alpha_l \boldsymbol{a}_{\mathrm{MS}}(\theta_l)\boldsymbol{a}_{\mathrm{BS}}^{\mathrm{H}}(\phi_l) \tag{4}$$

where ρ denotes the average path-loss between the BS and MS, and α_l is the complex gain of the l^{th} path. The variables $\phi_l \in [0, 2\pi]$ and $\theta_l \in [0, 2\pi]$ denote the l^{th} path's azimuth angles of departure or arrival (AoDs/AoAs) of the BS and MS, respectively. $\boldsymbol{a}_{\mathrm{BS}}(\phi_l)$ and $\boldsymbol{a}_{\mathrm{MS}}(\theta_l)$ are the antenna array response vectors at the

transmitter and receiver, respectively. If an uniform linear array (ULA) is assumed

$$\boldsymbol{a}_{\mathrm{BS}}(\phi_l)=\frac{1}{\sqrt{N_t}}\left[1, e^{\mathrm{j}(2\pi/\lambda)d\sin(\phi_l)},\ldots, e^{\mathrm{j}(N_t-1)(2\pi/\lambda)d\sin(\phi_l)}\right]^{\mathrm{T}} \tag{5}$$

$$\boldsymbol{a}_{\mathrm{MS}}(\theta_l)=\frac{1}{\sqrt{N_r}}\left[1, e^{\mathrm{j}(2\pi/\lambda)d\sin(\theta_l)},\ldots, e^{\mathrm{j}(N_r-1)(2\pi/\lambda)d\sin(\theta_l)}\right]^{\mathrm{T}} \tag{6}$$

where λ and d are the wavelength and the distance between antenna elements. The multipath channel model Eq. (4) can be written as

$$\boldsymbol{H}_{mck}=\boldsymbol{A}_{\mathrm{MS}}\boldsymbol{H}^{b}_{mck}\boldsymbol{A}^{\mathrm{H}}_{\mathrm{BS}} \tag{7}$$

where $\boldsymbol{H}^{b}_{mck}=\sqrt{\frac{N_tN_r}{\rho}}\,\mathrm{diag}(\alpha_1,\alpha_2,\ldots,\alpha_L)$. The matrices $\boldsymbol{A}_{\mathrm{BS}}\in\boldsymbol{C}^{N_t\times L}$ and $\boldsymbol{A}_{\mathrm{MS}}\in\boldsymbol{C}^{N_r\times L}$ contain the array response vectors in the directions ϕ_l and θ_l, i.e.

$$\boldsymbol{A}_{\mathrm{BS}}=[\boldsymbol{a}_{\mathrm{BS}}(\phi_1),\ldots,\boldsymbol{a}_{\mathrm{BS}}(\phi_L)] \tag{8}$$

$$\boldsymbol{A}_{\mathrm{MS}}=[\boldsymbol{a}_{\mathrm{MS}}(\theta_1),\ldots,\boldsymbol{a}_{\mathrm{MS}}(\theta_L)] \tag{9}$$

mmWave channels are expected to have limited scattering, therefore, a small number of propagation paths L is assumed.

Assume that the AoAs and AoDs are taken from a uniform grid of N points, with $N\gg L$. i.e., $\phi_l,\theta_l\in\{0,2\pi/N,\ldots,2\pi(N-1)/N\}$, $l=1,\ldots,L$. We define two dictionary matrices $\boldsymbol{A}_{\mathrm{MSD}}=[\boldsymbol{a}_{\mathrm{MS}}(\phi_1)\ldots\boldsymbol{a}_{\mathrm{MS}}(\phi_N)]$ and $\boldsymbol{A}_{\mathrm{BSD}}=[\boldsymbol{a}_{\mathrm{BS}}(\theta_1)\ldots\boldsymbol{a}_{\mathrm{BS}}(\theta_N)]$, with the associated array response vector in these directions. Neglecting the grid quantization error, we can represent $\boldsymbol{H}_{mck}$ in terms of a L-sparse matrix $\boldsymbol{H}^{v}_{mck}\in\boldsymbol{C}^{N\times N}$ containing the path gains of the quantized angles

$$\boldsymbol{H}_{mck}=\boldsymbol{A}_{\mathrm{MSD}}\boldsymbol{H}^{v}_{mck}\boldsymbol{A}^{\mathrm{H}}_{\mathrm{BSD}} \tag{10}$$

This representation provides a discretized approximation of the channel response that reduces the task of estimating $\boldsymbol{H}_{mck}$ to that of detecting some non-zero coefficients in the virtual channel matrix $\boldsymbol{H}^{v}_{mck}$ [19]. Vectorizing the channel matrix $\boldsymbol{H}_{mck}$, we have

$$\mathrm{vec}(\boldsymbol{H}_{mck})=(\boldsymbol{A}^{*}_{\mathrm{BSD}}\otimes\boldsymbol{A}_{\mathrm{MSD}})\,vec(\boldsymbol{H}^{v}_{mck})=(\boldsymbol{A}^{*}_{\mathrm{BSD}}\otimes\boldsymbol{A}_{\mathrm{MSD}})\,\boldsymbol{z}_{mck} \tag{11}$$

where $\boldsymbol{z}_{mck}=\mathrm{vec}(\boldsymbol{H}^{v}_{mck})$ is a $N^2\times 1$ sparse vector with L non-zero entries. We define the $N_tN_r\times N^2$ sparse matrix of the channel $\boldsymbol{\Psi}=\boldsymbol{A}^{*}_{\mathrm{BSD}}\otimes\boldsymbol{A}_{\mathrm{MSD}}$. Each column of $\boldsymbol{\Psi}$ is of the form $\boldsymbol{a}^{*}_{\mathrm{BS}}(\theta)\otimes\boldsymbol{a}_{\mathrm{MS}}(\varphi)$.

4 Interference suppression based on compressive sensing

Although the mmWave path loss reduces the intensity of the received interference greatly, the interference in the UDN is up to tens or even hundreds. The performance of mmWave cellular systems is obviously degraded by a large number of interfering cells. The increase of interference results in high computational complexity of the interference suppression algorithm. To address this problem, we propose compressive domain interference suppression in UDN. The compressive domain interference suppression scheme combines the interference suppression and CS. For the original signal that contains a large amount of interference, CS technology is used to transform high-dimension signal into low-dimension signal, as shown in Fig. 1. Note that $N\gg M$. Then, we conduct interference suppression on the signal after dimension reduction.

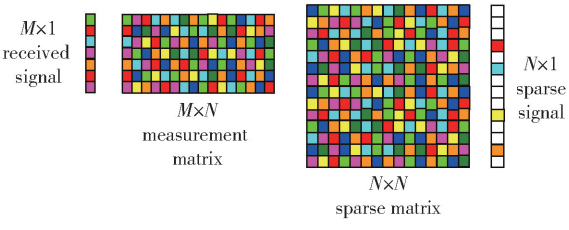

Fig. 1 Principle of CS

In this section, the CS-based interference suppression scheme is proposed for UDN. Firstly, measurement and sparse matrices are designed by exploiting the sparsity of millimeter wave channels. Then, we propose an oblique projection interference suppression scheme to suppress the interference in the compressed domain. Finally, we reconstruct the useful signal after interference suppression.

4.1 Construct the measurement matrix

Since the path loss for non-line-of-sight paths is much larger than that for line-of-sight paths, the mmWave massive channels appear the obvious sparsity. Moreover, by exploiting the sparsity of mmWave channels, we construct the measurement

matrix $\boldsymbol{\Phi}$. Specifically, we assume the channel state information $\boldsymbol{H}_{mck}$ is known. By vectorizing the $\boldsymbol{H}_{mck}$ $\boldsymbol{F}_{m,k}$, we have

$$\begin{aligned}\mathrm{vec}(\boldsymbol{H}_{mck}\boldsymbol{F}_{m,k}) &= \mathrm{vec}(\boldsymbol{A}_{\mathrm{MSD}}\boldsymbol{H}_{mck}^{v}\boldsymbol{A}_{\mathrm{BSD}}^{\mathrm{H}}\boldsymbol{F}_{m,k}) = \\ &(\boldsymbol{F}_{m,k}^{\mathrm{T}}\otimes\boldsymbol{I})(\boldsymbol{A}_{\mathrm{BSD}}^{*}\otimes\boldsymbol{A}_{\mathrm{MSD}})\boldsymbol{z}_{mck} = \boldsymbol{\Phi}_{m,k}\boldsymbol{\Psi}\boldsymbol{z}_{mck}\end{aligned} \quad (12)$$

where $\boldsymbol{\Phi}_{m,k} = \boldsymbol{F}_{m,k}^{\mathrm{T}} \otimes \boldsymbol{I}$ is the measurement matrix. Similar to the proof of Refs. [20 - 21], $\boldsymbol{\Phi}_{m,k}$ also satisfies a relaxed version of the restricted isometry property (RIP) to guarantee satisfactory performance of the sensing system. Therefore, according to Eq. (12), due to the sparsity of millimeter wave channels, we can use the measurement matrix $\boldsymbol{\Phi}_{m,k}$ and sparse matrix $\boldsymbol{\Psi}$ to compress the desired signal and interference signal. We defined $\tilde{\boldsymbol{x}}_{m,k} = \boldsymbol{z}_{mck}\boldsymbol{x}_{m,k}$. In the CS framework, Eq. (2) can be written as

$$\boldsymbol{y}_{ck} = \boldsymbol{\Phi}_{c,k}\boldsymbol{\Psi}\tilde{\boldsymbol{x}}_{c,k} + \sum_{n=1,n\neq k}^{K}\boldsymbol{\Phi}_{c,n}\boldsymbol{\Psi}\tilde{\boldsymbol{x}}_{c,n} + \sum_{m=1,m\neq c}^{M}\boldsymbol{\Phi}_{m}\boldsymbol{\Psi}\tilde{\boldsymbol{x}}_{m} + \tilde{\boldsymbol{n}}_{ck} \quad (13)$$

4.2 Cancel the interference based on compressive sensing

For UDN systems which have a large amount of interference, it is easier to find the optimal solution to hold interference cancellation by employing CS technology to transform high-dimensional sparse signals into low-dimension signals. However, when the number of interference is greatly increased for UDN systems, not only the computational complexity of interference suppression is greatly increased, but also the interference suppression of orthogonal projection operator is difficult to be obtained. The performance of the interference suppression algorithm based on orthogonal projection is significantly degraded. Therefore, the orthogonal projection interference suppression techniques in Ref. [22] are not practical due to the increase of interference for UDN. In contrast, oblique projection techniques in Ref. [23] provide a good trade off between performance and feasibility, and oblique projection scheme can be used for the desired signal and the interfering signal non-orthogonal cases, thus is preferred. In this section, we cancel interference in compress domain by constructing an oblique projection operator $\boldsymbol{E}$ that operates on the measurements $\boldsymbol{y}_{ck}$, while ensuring that the processed $\boldsymbol{y}_{ck}$ still contains enough information to complete the reconstruction of the desired signal $\tilde{\boldsymbol{x}}_{c,k}$.

Multiplying $\boldsymbol{E}$ by the received signal $\boldsymbol{y}_{ck}$ in Eq. (13), we have

$$\begin{aligned}\boldsymbol{E}\boldsymbol{y}_{ck} &= \boldsymbol{E}\boldsymbol{\Phi}_{c,k}\boldsymbol{\Psi}\tilde{\boldsymbol{x}}_{c,k} + \sum_{n=1,n\neq k}^{K}\boldsymbol{E}\boldsymbol{\Phi}_{c,n}\boldsymbol{\Psi}\tilde{\boldsymbol{x}}_{c,n} + \\ &\sum_{m=1,m\neq c}^{M}\boldsymbol{E}\boldsymbol{\Phi}_{m}\boldsymbol{\Psi}\tilde{\boldsymbol{x}}_{m} + \boldsymbol{E}\,\tilde{\boldsymbol{n}}_{ck} = \boldsymbol{E}\boldsymbol{\Phi}_{c,k}\boldsymbol{\Psi}\,\tilde{\boldsymbol{x}}_{c,k} + \boldsymbol{E}\,\tilde{\boldsymbol{n}}_{ck}\end{aligned} \quad (14)$$

The design of $\boldsymbol{E}$ is mainly based on knowledge of the location of the nonzero elements $\boldsymbol{z}$. The non-zero elements of the vector $\boldsymbol{z}$ are obtained by channel estimation. The $\boldsymbol{\Phi}_{r}$ is constructed from the columns of $\boldsymbol{\Phi}_{c,k}$ that corresponding to the positions of non-zero elements of $\boldsymbol{z}_{c,k}$. The $\boldsymbol{\Phi}_{I_1}$ is constructed from the columns of $\boldsymbol{\Phi}_{c,n}$ that corresponding to the positions of non-zero elements of $\boldsymbol{z}_{c,n}$. The $\boldsymbol{\Phi}_{I_2}$ is constructed from the columns of $\boldsymbol{\Phi}_{m}$ that corresponding to the positions of non-zero elements of $\boldsymbol{z}_{m}$. We assume that the $\boldsymbol{\Phi}_{c,k}$, $\boldsymbol{\Phi}_{c,n}$ and $\boldsymbol{\Phi}_{m}$ lie in the subspaces $\mathscr{R}(\boldsymbol{\Phi}_{J})$, $\mathscr{R}(\boldsymbol{\Phi}_{I_1})$ and $\mathscr{R}(\boldsymbol{\Phi}_{I_2})$, respectively. For the case of two interference subspaces $\mathscr{R}(\boldsymbol{\Phi}_{I_1})$ and $\mathscr{R}(\boldsymbol{\Phi}_{I_2})$, we denote

$$\mathscr{R}(\boldsymbol{\Phi}_{I}) = \mathscr{R}(\boldsymbol{\Phi}_{I_1}) \oplus \mathscr{R}(\boldsymbol{\Phi}_{I_2})$$

The purpose of the compressed domain interference suppression is to preserve the components of $\boldsymbol{y}_{ck}$ in the subspace $\mathscr{R}(\boldsymbol{\Phi}_{J})$ while completely eliminating the components of $\boldsymbol{y}_{ck}$ in another subspace $\mathscr{R}(\boldsymbol{\Phi}_{I})$ According to the oblique projection theorem [23], we can construct an oblique projection $\boldsymbol{E}_{\boldsymbol{\Phi}_J|\boldsymbol{\Phi}_I}$ from the direction of parallel the subspace $\mathscr{R}(\boldsymbol{\Phi}_{I})$ to the subspace $\mathscr{R}(\boldsymbol{\Phi}_{J})$ to achieve the purpose of eliminating interference. Obviously, the subspace of interference $\mathscr{R}(\boldsymbol{\Phi}_{I})$ and the subspace of the desired signal $\mathscr{R}(\boldsymbol{\Phi}_{J})$ are mutually disjoint. The oblique projection operator $\boldsymbol{E}_{\boldsymbol{\Phi}_J|\boldsymbol{\Phi}_I}$ onto $\mathscr{R}(\boldsymbol{\Phi}_{J})$ along $\mathscr{R}(\boldsymbol{\Phi}_{I})$ is expressed as

$$\boldsymbol{E}_{\boldsymbol{\Phi}_J|\boldsymbol{\Phi}_I} = \boldsymbol{\Phi}_{J}(\boldsymbol{\Phi}_{J}^{\mathrm{H}}\boldsymbol{P}_{\boldsymbol{\Phi}_I}^{\perp}\boldsymbol{\Phi}_{J})^{-1}\boldsymbol{\Phi}_{J}^{\mathrm{H}}\boldsymbol{P}_{\boldsymbol{\Phi}_I}^{\perp} \quad (15)$$

where $\boldsymbol{P}_{\boldsymbol{\Phi}_I}^{\perp} = \boldsymbol{I} - \boldsymbol{P}_{\boldsymbol{\Phi}_I} = \boldsymbol{I} - \boldsymbol{\Phi}_{I}(\boldsymbol{\Phi}_{I}^{\mathrm{H}}\boldsymbol{\Phi}_{I})^{-1}\boldsymbol{\Phi}_{I}^{\mathrm{H}}$ is the orthogonal projection operator. The two subspaces $\mathscr{R}(\boldsymbol{\Phi}_{J})$ and $\mathscr{R}(\boldsymbol{\Phi}_{I})$ are called the range space and

the null space of the projector.

The oblique projection operator has thefollowing properties

$$\boldsymbol{E}_{\boldsymbol{\Phi}_J|\boldsymbol{\Phi}_I}\boldsymbol{\Phi}_I = 0,\ \boldsymbol{E}_{\boldsymbol{\Phi}_J|\boldsymbol{\Phi}_I}\boldsymbol{\Phi}_J = \boldsymbol{\Phi}_J \tag{16}$$

According to the properties of oblique projection, we tailor interference suppression technology to efficiently eliminate interference. Specifically, based on the oblique projection operator $\boldsymbol{E}_{\boldsymbol{\Phi}_J|\boldsymbol{\Phi}_I}$, Eq. (13) can be written as

$$\boldsymbol{E}_{\boldsymbol{\Phi}_J|\boldsymbol{\Phi}_I}\boldsymbol{y}_{ck} = \boldsymbol{\Phi}_J\boldsymbol{\Psi}\tilde{\boldsymbol{x}}_{c,k} + \boldsymbol{E}_{\boldsymbol{\Phi}_J|\boldsymbol{\Phi}_I}\tilde{\boldsymbol{n}}_{ck} \tag{17}$$

From Eq. (16), it can be seen that interference is totally canceled, and meanwhilethe desired signal $\tilde{\boldsymbol{x}}_{c,k}$ can be preserved.

4.3 Sparse signal reconstruction

Given the measurement signal $\boldsymbol{y}_{ck}$ and the interference compression matrix $\boldsymbol{\Phi}_J$, the task of the signal reconstruction is to use a certain algorithm to reconstruct the desired signal $\tilde{\boldsymbol{x}}_{c,k}$. We can formulate the following problem to estimate $\tilde{\boldsymbol{x}}_{c,k}$

$$\min \|\boldsymbol{x}_{c,k}\|_1 \text{ s.t. } \|\boldsymbol{E}_{\boldsymbol{\Phi}_J|\boldsymbol{\Phi}_I}\boldsymbol{y}_{ck} - \boldsymbol{\Phi}_J\boldsymbol{\Psi}\tilde{\boldsymbol{x}}_{c,k}\| \leqslant \varepsilon \tag{18}$$

where ε is decided by the noise vector $\tilde{\boldsymbol{n}}_{ck}$. Although Eq. (17) is a convex optimization problem, its solution can be found at the expense of the computational complexity. Thus, there have been various low-complexity approaches to find approximate solutions including greedy algorithms. In particular, low complexity approaches are attractive for interference suppression in the compress domain. In Sect. 5 for simulations, we consider SWOMP algorithm in Ref. [24], which is one of greedy algorithms. The SWOMP algorithm can estimate the signal $\tilde{\boldsymbol{x}}_{c,k}$ in Eq. (17) from $\boldsymbol{y}_{ck}$ with known measurement matrix $\boldsymbol{\Phi}_J$. The following is the specific steps of the SWOMP algorithm.

Algorithm 1 SWOMP algorithm

Input: measurements $\boldsymbol{E}_{\boldsymbol{\Phi}_J|\boldsymbol{\Phi}_I}\boldsymbol{y}_{ck}$,
sensing matrix $\boldsymbol{\Phi}_J$,
threshold parameter α
number of iterations S

Initialize: iteration count $t = 0$,
residual vector $\boldsymbol{r}^0 = \boldsymbol{E}_{\boldsymbol{\Phi}_J|\boldsymbol{\Phi}_I}\boldsymbol{y}_{ck}$,
estimated support set $\Lambda^0 = \varnothing$

While $\|\boldsymbol{r}^t\|_2 > \delta$ and $t > S$ do

$k = k + 1$

(**Identification**) Calculate $\boldsymbol{u} = \text{abs}[\boldsymbol{\Phi}_J^{\mathrm{T}}\boldsymbol{r}^{t-1}]$ and select columns from $\boldsymbol{\Phi}_J$ based on elements in $\boldsymbol{u}$ that exceed the threshold $Th = \alpha\max\{\text{abs}(\boldsymbol{u})\}$. The indexes of the selected elements are added to J_0.

(**Augmentation**) $\Lambda^t = \Lambda^{t-1} \cup J_0$. if $\Lambda^t = \Lambda^{t-1}$, stop iterating

(**Estimation of**) $\hat{\boldsymbol{x}}_{c,k} = \arg\min_{\tilde{\boldsymbol{x}}_{c,k}} \|\boldsymbol{E}_{\boldsymbol{\Phi}_J|\boldsymbol{\Phi}_I}\boldsymbol{y}_{ck} - \boldsymbol{\Phi}_J^{\Lambda^t}\tilde{\boldsymbol{x}}_{c,k}\| = ((\boldsymbol{\Phi}_J^{\Lambda^t})^{\mathrm{T}}\boldsymbol{\Phi}_J^{\Lambda^t})^{-1}(\boldsymbol{\Phi}_J^{\Lambda^t})^{\mathrm{T}}\boldsymbol{E}_{\boldsymbol{\Phi}_J|\boldsymbol{\Phi}_I}\boldsymbol{y}_{ck}$

(**Residual Update**) $\boldsymbol{r}^t = \boldsymbol{E}_{\boldsymbol{\Phi}_J|\boldsymbol{\Phi}_I}\boldsymbol{y}_{ck} - \boldsymbol{\Phi}_J^{\Lambda^t}\boldsymbol{\Psi}\hat{\boldsymbol{x}}_{c,k} = \boldsymbol{E}_{\boldsymbol{\Phi}_J|\boldsymbol{\Phi}_I}\boldsymbol{y}_{ck} - \boldsymbol{\Phi}_J^{\Lambda^t}((\boldsymbol{\Phi}_J^{\Lambda^t})^{\mathrm{T}}\boldsymbol{\Phi}_J^{\Lambda^t})^{-1}(\boldsymbol{\Phi}_J^{\Lambda^t})^{\mathrm{T}}\boldsymbol{E}_{\boldsymbol{\Phi}_J|\boldsymbol{\Phi}_I}\boldsymbol{y}_{ck}$

end

Output: $\hat{\boldsymbol{x}}_{c,k}$

5 Simulationresults

In this section, Monte Carlo simulations are carried out in order to evaluate the system performance of our proposed interference suppression algorithm. There are one macro cell and three pico cells deployed within the coverage area of macro cell. The macro user equipments (UEs) and pico UEs are distributed uniformly. The macro sector and the pico cells are

equipped with 8 and 2 transmit antennas, respectively. The macro cell serves 2 UEs and each pico cell is serving one UE. The other simulation parameters are shown in Table 2. In the simulation, three interference suppression schemes are considered: oblique projection, orthogonal projection, interference suppression. By employing oblique projection or orthogonal projection interference suppression based on CS, we cancel out the intra-cell and inter-cell interference in the measurements $\boldsymbol{y}_{ck}$ and directly recover the desired signal $\hat{\boldsymbol{x}}_{c,k}$ using the SWOMP algorithm.

Table 2 Simulation parameter

Parameter	Value
Channel model	3rd generation partnership project (3GPP) spatial channel model (SCM) Micro Urban
Number of Macro BS	4
Number of small cells	12
User distribution	Uniformly distributed
Simulation model	Monte Carlo (2 000 runs)
Measured value M	100
Reconstruction algorithm	SWOMP algorithm

Fig. 2 compares the performance of the proposed scheme relative to the CS-based orthogonal projection algorithm in Ref. [12] and the non-CS based interference mitigation algorithm under the same simulation conditions. For the method in Ref. [12], the premise of eliminating interference is that the subspace of the interference signal is orthogonal to the subspace of the desired signal. For UDN system which has a large amount of interference, this method is difficult to eliminate the influence of interfering signals in the received signal while ensuring that the structure of the desired signal is not affected. In contrast, oblique projection interference suppression techniques that can be used for non-orthogonal situations of desired and interfering signals provide a good trade off between performance and feasibility. In the non-CS based interference mitigation algorithm, the interference is assumed to be known at the receiver. The conventional least square method is used to recover $\hat{\boldsymbol{x}}_{c,k}$ without further knowledge of the support of $\hat{\boldsymbol{x}}_{c,k}$. By setting $M = 100$ and using SWOMP recovery algorithms, simulation results indicate that the proposed method achieves much better performance than the CS based orthogonal projection algorithm and the non-CS based interference mitigation algorithm. The non-CS based interference mitigation algorithm is worse than CS-based algorithms.

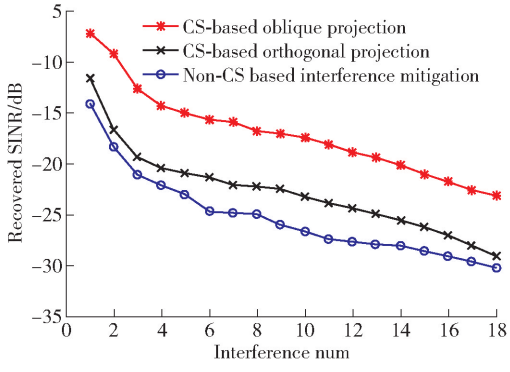

Fig. 2 SINR of three different interference suppression under different numbers of interference

Fig. 3 compares the effect of varying recovery algorithms on the oblique projection interference suppression scheme, including orthogonal matching pursuit (OMP) in Ref. [25], compressive sampling matching pursuit (CoSaMP) in Ref. [26], basis pursuit de-noising (BPDN) in Ref. [27], sparsity adaptive matching pursuit (SAMP) in Ref. [28], SWOMP, subspace pursuit (SP) in Ref. [29], regularized orthogonal matching pursuit (ROMP) in Ref. [30], and generalized orthogonal matching pursuit (GOMP) in Ref. [31]. In all cases, the

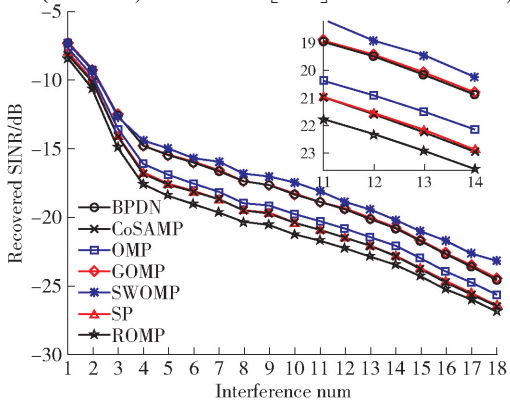

Fig. 3 SINR using different reconstruction algorithms under different numbers of interference

SWOMP algorithm outperform other recovery algorithms obviously, since the SAMP algorithm reconstructs the signal without knowing the sparsity of the signal.

6 Conclusions

To avoid the performance degradation caused by the intricate interference, we proposea CS-based interference suppression for UDN. Interference compression does not require coordinated transmission or resource scheduling of multiple cells, which avoids degradation of compression interference performance due to channel measurements and feedback requirements of neighboring cells, backhaul delay and centralized processing delays. Specifically, we exploit the sparsity of mmWave channels and regard it as the spare basis of CS framework. The interference suppression in compressive domain reduces the computational complexity. Finally, the SWOMP is used to formulate the data detection as the signal reconstruction in compressive domain. Simulation results show that the proposed algorithm achieves a significant performance over other existing interference suppression algorithms in UDN.

Acknowledgements

This work was supported by National Science and Technology Major Project (2016ZX03001016), Innovation Team Project of Shaanxi Province (2017KCT-30-02), National Natural Science Foundation of China (6187012068).

References

1. Gao Z, Dai L L, Mi D, et al. MmWave massive MIMO based wireless backhaul for 5G ultra-dense network. IEEE Wireless Communications, 2015, 22(5): 13 – 21
2. Ge X H, Tu S, Mao G Q, et al. 5G ultra-dense cellular networks. IEEE Wireless Communications, 2016, 23(1): 72 – 79
3. Kamel M, Hamouda W, Youssef A. Ultra-dense networks: a survey. IEEE Communications Surveys and Tutorials, 2016, 18(4): 2522 – 2545
4. An J P, Yang K, Wu J S, et al. Achieving sustainable ultra-dense heterogeneous networks for 5G. IEEE Communications Magazine, 2017, 55(12): 84 – 90
5. Hao P, Yan X, Yuan Y F, et al. Ultra dense network: challenges, enabling technologies and new trends. China Communications, 2016, 13(2): 30 – 40
6. Shgluof I, Ismail M, Nordin R. Semi-clustering of victim-cells approach for interference management in ultra-dense femtocell networks. IEEE Access, 2017(5): 9032 – 9043
7. Chen Y, Yang Z H, Zhang H T. Opportunistic-based dynamic interference coordination in dense small cells deployment. 2017 IEEE 28th Annual International Symposium on Personal, Indoor, and Mobile Radio Communications (PIMRC), Oct 8 – 13, 2017, Montreal, QC, Canada, 2017: 1 – 5
8. Cao J Q, Peng T, Qi Z Q, et al. Interference management in ultra-dense networks: a user-centric coalition formation game approach. IEEE Transactions on Vehicular Technology, 2018, 67(6): 5188 – 5202
9. Munir H, Hassan S A, Pervaiz H, et al. A game theoretical network-assisted user-centric design for resource allocation in 5G heterogeneous networks. 2016 IEEE 83rd Vehicular Technology Conference (VTC Spring), May 15 – 18, 2016, Nanjing, China, 2016: 1 – 5
10. Zaidi S, Affes S, Vilaipornsawai U, et al. Wireless access virtualization strategies for future user-centric 5G network. 2016 IEEE Globecom Workshops (GC Wkshps), Dec 4 – 8, 2016, Washington, DC, USA, 2016: 1 – 7
11. Liu Y M, Li X, Ji H, et al. Grouping and cooperating among access points in user-centric ultra-dense networks with non-orthogonal multiple access. IEEE Journal on Selected Areas in Communications, 2017, 35(10): 2295 – 2311
12. Davenport M A, Boufounos P T, Baraniuk R G. Compressive domain interference cancellation. Proceedings of the Workshop: Signal Processing with Adaptive Sparse Structured Representation (SPARS), Saint-Malo, France, 2009: 1 – 5
13. Lu X D, Yang P C, Li D J, et al. Interference cancellation based on compressive sensing for passive coherent radar (PACOR). 2015 IEEE Radar Conference (RadarCon), May 10 – 15, 2015, Arlington, VA, USA, 2015: 0527 – 0532
14. Gomaa A, Al-Dhahir N. Compressive-sensing-based approach for NBI cancellation in MIMO-OFDM. 2011 IEEE Global Telecommunications Conference-GLOBECOM 2011, Dec 5 – 9, 2011, Kathmandu, Nepal, Houston, TX, USA, 2011: 1 – 5
15. Liu J C, Liu A, Lau V K N. Compressive interference mitigation and data recovery in cloud radio access networks with limited fronthaul. IEEE Transactions on Signal Processing, 2017, 65(6): 1437 – 1446
16. Gowda N M, Kannu A P. Interferer identification in HetNets using compressive sensing framework. IEEE Transactions on Communications, 2013, 61(11): 4780 – 4787
17. Rappaport T, Tamir J, Murdock J, et al. Cellular broadband millimeter wave propagation and angle of arrival for adaptive beam steering systems. 2012 IEEE Radio and Wireless Symposium, Jan 15 – 18, 2012, Santa Clara, CA, USA, 2012: 151 – 154
18. Murdock J, Ben-Dor E, Tamir J, et al. A 38 GHz cellular outage study for an urban outdoor campus environment. 2012 IEEE Wireless Communications and Networking Conference (WCNC), Apr 1 – 4, 2012, Shanghai, China, 2012: 3085 – 3090
19. Bajwa W U, Haupt J, Sayeed A M, et al. Compressed channel sensing: anewapproach to estimating sparse multipath channels. Proceedings of the IEEE, 2010, 98(6): 1058 – 1076
20. Alkhateeb A, El A O, Leus G, et al. Channel estimation and hybrid precoding for millimeter wave cellular systems. IEEE Journal of Selected Topics in Signal Processing, 2014, 8(5): 831 – 846
21. Méndez-Rial R, Rusu C, González-Prelcic N, et al. Hybrid MIMO

architectures for millimeter wave communications: phase shifters or switches? IEEE Access, 2016(4): 247 – 267

22. Jiang J, Chen Y. Interference cancellation based on compressive sensing framework for ultra dense network. 2017 IEEE 17th International Conference on Communication Technology (ICCT), Oct 27 – 30, 2017, Chengdu, China, 2017: 810 – 814
23. Behrens R T, Scharf L L. Signal processing applications of oblique projection operators. IEEE Transactions on Signal Processing, 1994, 42(6): 1413 – 1424
24. Blumensath T, Davies M E. Stagewise weak gradient pursuits. IEEE Transactions on Signal Processing, 2009, 57(11): 4333 – 4346
25. Tropp J A, Gilbert A C. Signal recovery from random measurements via orthogonal matching pursuit. IEEE Transactions on Information Theory, 2007, 53(12): 4655 – 4666
26. Needell D, Tropp J A. CoSaMP: iterative signal recovery from incomplete and inaccurate samples. Applied and Computation Harmonic Analysis, 2009, 26: 301 – 321
27. Nowak R D, Wright S J. Gradient projection for sparse reconstruction: application to compressed sensing and other inverse problems. IEEE Journal of Selected Topics in Signal Processing, 2007, 1(4): 586 – 597
28. Do T T, Gan L, Nguyen N, et al, Sparsity adaptive matching pursuit algorithm for practical compressed sensing. 2008 42nd Asilomar Conference on Signals, Systems and Computers, Oct 26 – 29, 2008, Pacific Grove, CA, USA, 2008: 581 – 587
29. Dai W, Milenkovic O. Subspace pursuit for compressive sensing signal reconstruction. IEEE Transactions on Information Theory, 2009, 55(5): 2230 – 2249
30. Needell D, Vershynin R. Uniform uncertainty principle and signal recovery via regularized orthogonal matching pursuit. Foundations of Computational Mathematics, 2009, 9(3): 317 – 334
31. Wang J, Kwon S, Shim B. Generalized orthogonal matching pursuit. IEEE Transactions on Signal Processing, 2012, 60(12): 6202 – 6216

(Editor: Ai Lisha)